A FIBER-OPTIC AIRCRAFT LIGHTNING CURRENT MEASUREMENT SENSOR

Truong X. Nguyen, Jay J. Ely and George N. Szatkowski
NASA Langley Research Center
Hampton, VA 23681 U.S.A.
truong.x.nguyen@nasa.gov

ABSTRACT

A fiber-optic current sensor based on the Faraday Effect is developed for aircraft installations. It can measure total lightning current amplitudes and waveforms, including continuing current. Additional benefits include being small, light-weight, non-conducting, safe from electromagnetic interference, and free of hysteresis and saturation. The Faraday Effect causes light polarization to rotate in presence of magnetic field in the direction of light propagation. Measuring the total induced light polarization change yields the total current enclosed.

The system operates at 1310nm laser wavelength and can measure approximately 300 A - 300 kA, a 60 dB range. A reflective polarimetric scheme is used, where the light polarization change is measured after a round-trip propagation through the fiber. A two-detector setup measures the two orthogonal polarizations for noise subtraction and improved dynamic range. The current response curve is non-linear and requires a simple spline-fit correction.

Effects of high current were achieved in laboratory using combinations of multiple fiber and wire loops. Good result comparisons against reference sensors were achieved up to 300 kA. Accurate measurements on a simulated aircraft fuselage and an internal structure illustrate capabilities that maybe difficult with traditional sensors. Also tested at a commercial lightning test facility from 20 kA to 200 kA, accuracy within 3-10% was achieved even with non-optimum setups.

ACRONYMS AND SYMBOLS

(a),(b),(c): Detector output voltages
A : Ampere
B : Magnetic flux density
c : Speed of light
CT : Current Transformer
DC : Direct-current
E : Polarization
H : Magnetic field
I : Enclosed current
L : Fiber interaction length
msec: Millisecond
MM: Multi-mode
n : Index of refraction
N : Product of no. of closed fiber loops and no. of wire turns
PM : Polarization-maintaining (fiber)
SM : Single-mode
SLD: Superluminescent diode
t : Transit time
V : Verdet constant
ϕ : Polarization Rotation angle
μ_0 : Free space permeability

INTRODUCTION

Growing applications of composite materials in commercial aircraft manufacturing has significantly increased the risk of aircraft damage due to lightning attachment. A risk mitigation strategy involves determining lightning current intensities and distributions on the aircraft from which damage risks could be inferred. Suitable onboard current sensors can be used to measure current intensities and paths during a strike.

For aircraft lightning current measurement, it is desirable to have a current sensor that measures total lightning current directly, operates down to (near) DC frequency, conforms to aircraft structures, has large dynamic range, and is light-weight and non-conductive (for safety reasons). These characteristics are difficult to achieve with traditional sensors. Ferromagnetic-core current transformers, solid state current sensors and shunt resistors suffer from one or more limitations such as weight, sensitivity, range, hysteresis, saturation, or installation difficulties. Outputs from B-Dot sensor, I-Dot sensor and Rogowski coil variants must be integrated to yield desired parameters, and accuracy can be a concern at very low frequencies where most of the lightning energy is concentrated. B-Dot and I-Dot sensors were used on the NASA F-106 in the Storm Hazard Program in the 1980's [1]. These traditional sensors can satisfy only a few of the desirables previously listed.

Optical current sensors have been under development for decades. They are beginning to be commercialized, mostly for the power generation and distribution industries. The sensors typically rely on Faraday rotation, in which the light's polarization plane rotates when the medium is exposed to a magnetic field. The amount of rotation depends on the optical medium, the wavelength, and is proportional to the interaction length and the intensity of the magnetic field component in the direction of light propagation.

There are two main groups of optical sensing elements: crystal/bulk-glass based and fiber based. Crystal/bulk-glass based sensors can choose from an extensive list of available materials with wide ranges of optical properties. They can have high bandwidth, small size and be immune to vibration. They generally measure only local current or magnetic fields. This type of sensor has been proposed for lightning sensing on windmill structures [2].

The sensor discussed in this paper is optical fiber based. The sensor can be highly flexible, and by forming closed loop(s) around a structure, the total enclosed current can be measured. Fig. 1 illustrates fiber loops measuring total lightning current flowing through aircraft structures of interest. By comparing amplitudes and timing at different locations, current flow paths may be determined. In contrast, the dots in the same figure illustrate traditional field sensors, such as B-Dot, for sampling local B-fields. An inverse problem must be solved for the specific aircraft to approximate total current amplitudes [1,3].

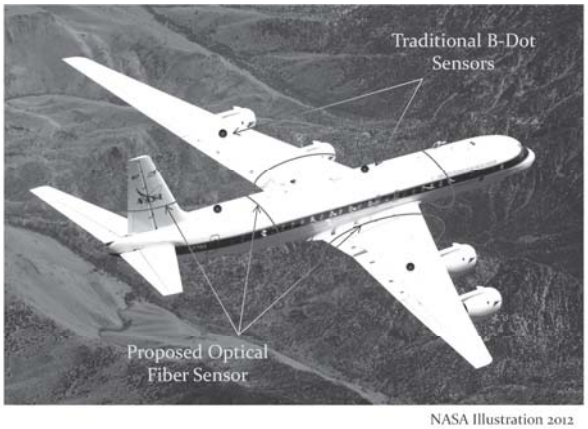

Fig. 1. Illustration of fiber-optic current sensors on aircraft.

There are many important advantages to a fiber optic current sensor. These include the abilities to conform to large, complex structure geometries. It is self-integrating, thus the output is directly related to the total current. The sensor is also small, lightweight, immune from interference, and free of hysteresis and saturation. The sensing fiber is also safe from lightning hazards and can be routed directly into the aircraft fuselage.

The sensor is highly suitable for applications such as in-flight lightning parameters characterization, and can enable inferred-damage assessments after a lightning strike. In addition, it can also measure internal currents, i.e., inside the fuselage and wings, for system health monitoring, lightning transfer function or certification purposes. Use on lightning towers and windmill structures is also possible.

The material choice for optical fiber is limited - most commonly-available fibers are based on silica. The Faraday Effect in silica is weak, which makes it ideal for large currents in lightning. Measurement sensitivity and range may be optimized by choosing an appropriate laser wavelength. Temperature and bend/vibration sensitivities could be of concern depending on designs and accuracy requirements. The fiber is also fragile and needs suitable protection.

In the remainder of the paper, basic sensor operation, design, and bandwidth and laboratory test results are discussed. Demonstrations measuring large current up to 200 kA are reported. In addition, measurement results on a large aluminum cylinder simulating an aircraft fuselage, and on an internal structure to the cylinder, are compared against reference sensors.

Two other sensor systems of similar design, operating at laser wavelengths 850nm and 1550nm, were evaluated measuring rocket-triggered lightning in the summers of 2011 and 2012. Their results are reported in a parallel paper [4]. Faraday-rotation fiber-optic current sensor is simply referred to as Faraday sensor in this paper.

FIBER-OPTIC CURRENT SENSOR SOLUTION

Due to the Faraday Effect, light polarization in an optical medium rotates when the medium is exposed to a magnetic field in the direction of light propagation. The amount of rotation depends on

the material and the strength of the magnetic field component in the propagation direction. The effect in the fiber is illustrated in Fig. 2. The polarization plane rotation, in radians, is [5-9]:

$$\phi = V \int \boldsymbol{B} \cdot d\boldsymbol{l} = \mu_0 V \int \boldsymbol{H} \cdot d\boldsymbol{l}\,, \tag{1}$$

where μ_0 is the free-space permeability; V is the Verdet constant in radians/(meter·Tesla); $\mu_0 V$ is the combined permeability Verdet constant (radians/ampere); $\boldsymbol{B}$ is magnetic flux density in Tesla (T); length $\boldsymbol{l}$ (in meters) is the light and magnetic field interaction path length; and $\boldsymbol{H}$ is the magnetic field (amperes/meter). For a fiber forming N closed loops around a conductor carrying current **I** (ampere), applying Ampere's law yields

$$\begin{aligned} \phi &= \mu_0 V \oint \boldsymbol{H} \cdot d\boldsymbol{l}\,, \\ &= \mu_0 VNI. \end{aligned} \tag{2}$$

Thus, the rotation angle is directly proportional to the current and the number of loops. Measuring the rotation angle can directly result in current. The sensor is self-integrating, and no additional integration is needed.

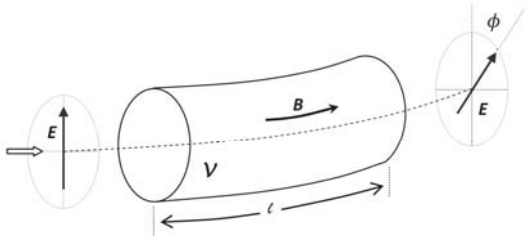

Fig. 2. Faraday Effect in optical fiber.

SENSOR DESCRIPTION

The polarization measurement scheme is illustrated in Fig. 3. The scheme measures the polarization change induced by current. A linearly polarized light from a super-luminescence diode (SLD) laser is generated at locations labeled *1*, *2*. Half of the power is transmitted through the non-polarizing beam splitter (NBS) at *3* to the sensing fiber at *4*. The sensing fiber forms closed loops around the current carrying conductor at *5*. A Faraday mirror at *6* rotates the reflected light polarization by 90º relative to the incident light. This helps cancel fiber bend/stress induced effects makes the sensor less sensitive to bending. The reflected light traces back through the fiber to *3*, at which half of the power is reflected through the half-wave plate (HWP) at *7* toward the polarizing beam splitter (PBS) at *8*. Exiting the PBS, light power in the two orthogonal polarizations are measured by two photo-detectors D1 and D2 at *9*. The HWP helps rotate and align the initial polarization incident on the PBS. Ideally, at zero current the incident polarization should be at 45º relative to the PBS's two orthogonal principle polarization axes, so that beam power is divided equally between the two optical detectors at *9*. A balanced detector, with two built-in matched detectors, is used in place of two separate detectors. This helps cancel common-mode noise between the two outputs and improves overall noise performance.

This setup is referred to as a reflective scheme, since a mirror is incorporated. Using this scheme in combination with a Faraday mirror, as light travels through the fiber twice the non-reciprocal Faraday rotation due to current is doubled while stress-induced effects are subtracted [6].

The responses at the two detectors should ideally be $(a),(b)=0.5*(1\pm sin(4\mu_0 VNI))$ for reflective scheme. Mathematic operation *difference-over-sum*, $(c) = \frac{(a-b)}{(a+b)}$, yields

$$(c) = \sin(4\mu_0 VNI), \text{ or} \tag{3}$$

$$NI = \frac{1}{4\mu_0 V}\sin^{-1}(c), \tag{4}$$

where NI is the number of loops N times the current I, and $\mu_0 V$ = 1.01^{-6} rad/A 1310nm [5]. The *difference* operation is actually performed with the balanced detector that yields only one output voltage waveform. The *sum* operation is performed separately and does not change with current.

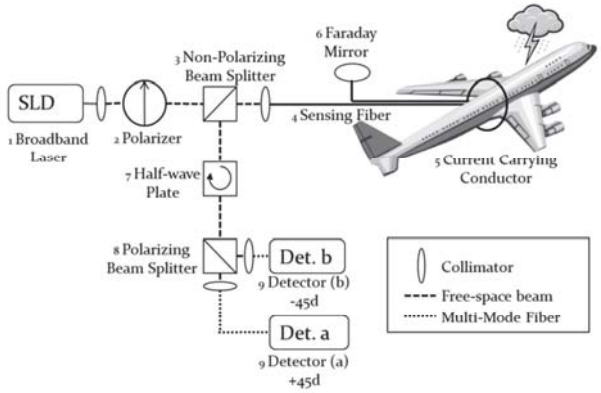

Fig. 3. Reflective polarimeric scheme with dual detectors.

It is important that light's state-of-polarization is maintained in the fiber during light transit. Fiber twisting helps hold the state-of-polarization that otherwise would be destroyed in a typical single-mode fiber. The system uses a 15m-long *spun* polarization-maintaining (PM) fiber [7]. Spun PM fiber is the result of twisting a PM fiber during manufacturing. The twist rate is about 5 mm per turn for this fiber.

Fig. 4 describes ideal responses, with the curves labeled (a) and (b) being voltage outputs from the two optical detectors. While either can be used to determine current, performing *difference-over-sum* operation $(c) = \frac{(a-b)}{(a+b)}$ would yield a response that is more sensitive (higher slope), with zero crossing at zero current, and has larger dynamic range from common-mode noise subtraction. Current is computed from (*c*) using eq. (3).

The typical operating range is in the region where curve (*c*) increases monotonically in Fig. 4, or about -350 kA to +350 kA. Non-ideal medium and components in a practical system distorts the curves, and the range is slightly reduced to about +/- 300 kA.

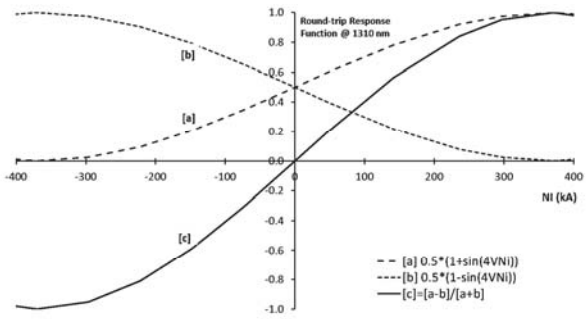

Fig. 4. Ideal sensor responses at 1310 nm.

Sensor Response and Data Correction

The system was measured in laboratory and compared with reference sensors that include a Rogowski coil (with an electronic integrator), and a ferrite-based Pearson™ current transformer (CT). Fig. 5 compares the three sensors by plotting current from the Faraday sensors on the vertical axis against current from other reference sensors on the horizontal axis.

Theoretically, the Faraday sensor data would fall on the straight diagonal line labeled as "ideal". In this setup, the data follow the curves labeled "uncorrected". This response is due to the reduced sensitivity in the fiber and depolarization from non-ideal fiber medium and optical components. Additional details characterizing light propagation in spun fiber can be found in [7].

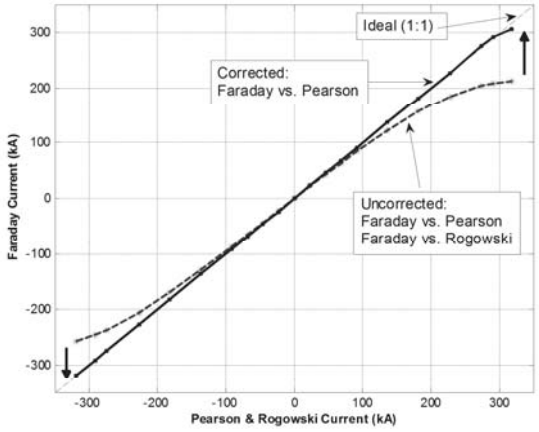

Fig. 5. The 1310nm system's response curve, corrected and un-corrected.

To correct for both the reduced sensitivity and the non-linear response, a simple spine-fit "correction" function is developed from Fig. 5 that maps the Faraday sensor response to the "ideal" curves. The "corrected" response curve aligns well with the ideal diagonal lines shown in the same plots. The same correction function can then be applied to subsequent measurements to achieve the correct results. An alternative to curve-fitting is interpolation. Neither approach is perfect, as some small error may remain.

Fig. 6 illustrates a typical setup to achieve Faraday rotation levels associated with high current. Multiple fiber loops and wire turns are used to amplify the Faraday rotation beyond that produced by a single conductor on a single fiber loop. The amplification factor is simply the product of the numbers of fiber loops and wire turns used. In the illustration, with 49 being the number of wire turns, and 4 being the of fiber loops, the rotation angle amplification is 49 x 4 = 196. Since the reference Rogowski coil and the Pearson current transformer (CT) only measure current on one wire-turn, their results are numerically scaled by the same factor, 196, for comparison. This practice is widely accepted and used in optical current sensing. Additional details have been previously discussed in [10].

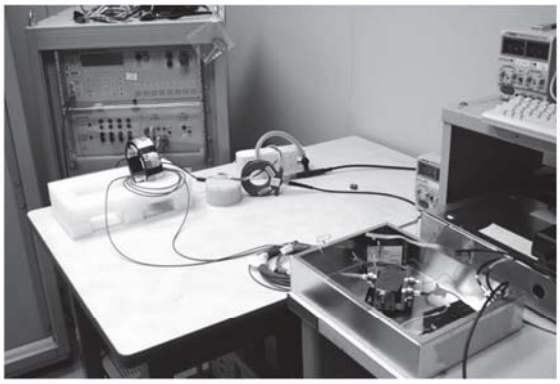

Fig. 6. Optical effects of high current are achieved with a multi-turn coil and multiple fiber loops.

Fig. 7 illustrates the Faraday sensor measurements against the reference sensors for peak current*loops products (N*I) = 23 kA and 200 kA, with N being the product of the number of wire-turns and number of fiber loops. Good result comparisons were achieved. Though not shown, similarly good results were achieved for N*I from 300 A to 300 kA. Using a coil with high number of turns (to help achieve high current effects) can distort the injected waveform, as can be seen comparing Fig. 7(ii) against Fig. 7(i). The pulse in 7(ii) width widens considerably. Alternatively, using a high number of fiber loops does not affect the current waveform, but would require a longer sensing fiber.

Sensor Bandwidth

Bandwidth of a sensor system is limited by the lowest bandwidth of its components. For the fiber sensor component, it is limited by the light transit time in the interaction length of the fiber. This bandwidth limitation is to ensure the total transit time is much faster than the signal change rate. The fiber interaction length in the bandwidth consideration includes the round-trip length around the conductor and includes the length to and from the Faraday sensor. The 3-dB sensor bandwidth (BW) is [5,6]: $BW \approx \frac{0.44}{t} \approx 0.44c/nl$, where t is transit time, c is the speed of light in free space, n is the index of refraction in fiber material (n=1.5), and l is the interaction length (double of fiber length for the reflective scheme described).

Table 1 computes the maximum fiber length and structure dimensions for different bandwidths. Aircraft thin structures may include wings and tail

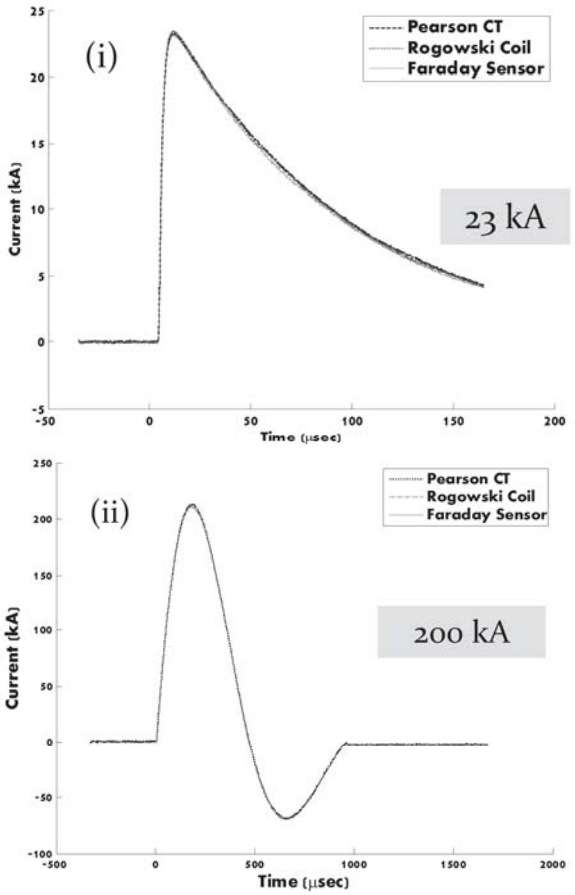

Fig. 7. Good comparison achieved in laboratory setups using (i) 2 wire turns and 50 fiber loops, and (ii) 49-turn coil and one fiber loop.

surfaces, while round structures may include fuselage, engine, etc. For reference, fuselage outside diameters for various aircraft (averaging the width and height) include: Airbus A380: 7.8 m; Boeing 767: 5.3 m; Boeing 737: 3.8 m. Assuming most of the damaging lightning energy is contained in spectrum far below 1-2 MHz, the table shows there is sufficient sensor bandwidth

Table 1. Sensor Bandwidth vs. Dimension.

3-dB Bandwidth (MHz)	Max. Fiber Length (m)	Max Thin Structure Dimension (m)	Max. Round Structure Diameter (m)
1	44	22	14
2	22	11	7
4	11	5.5	3.5
10	4.4	2.2	1.4
20	2.2	1.1	0.7

even for the fuselage of the largest passenger aircraft, the Airbus A380.

LARGE CURRENT MEASUREMENT WITH ONE FIBER LOOP

The sensor system was evaluated for large current measurement with just one fiber loop over one conductor, as it would be the case if the sensor is installed external to an aircraft fuselage. Performed at a commercial lightning test facility, this test was in coordination with a separate effort to evaluate lightning damage to composite panels and their interactions. Standard lightning test waveforms D, B and C were used [11] with peak amplitudes from 20 kA to 200 kA.

Fig. 8 illustrates the test setup, with the Faraday sensor fiber loop around the flat-plate return conductor. In an optimum setup, both ends of the fiber loop would be co-routed and exit the test zone with high magnetic field. Due to space limitation associated with cable routings, only one end of the fiber was routed to the optical box inside the cabinet (on left side). The other end and the remaining fiber were coiled up and put aside. As shown, a section of the fiber was unpaired and routed through strong magnetic fields near the test zone. Thus, some error in the data was anticipated.

Fig. 9 compares the results for 100 kA and 200 kA peak current against reference sensors. One reference sensor (data provided by the test facility) provided only component D data, even though all components D, B and C were present. The other reference was a sum of the outputs from four current transformers measuring currents exiting the sides of the test composite panels. This data sum included all mentioned test components. Fig. 9 shows the comparisons are

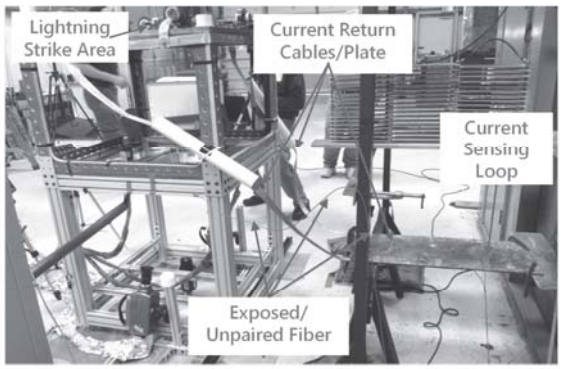

Fig. 8. Measuring large current (on flat structure) with just one fiber loop.

reasonably good, and that the Faraday sensor captures data that included all components. As expected, there are errors in the comparisons due to the non-optimum sensor installation. However, the errors are only about 3-10% depending on how the unpaired fiber section was routed. These results prove that the Faraday sensor can measure large current using just one fiber loop over one conductor.

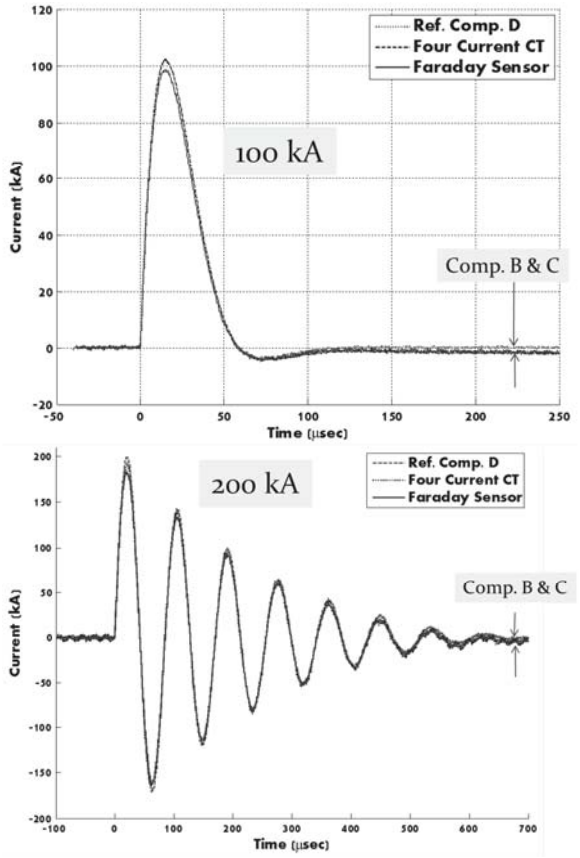

Fig. 9. Reasonable comparison achieved measuring large current (100 kA and 200 kA) with one fiber loop despite imperfect setup.

LARGE STRUCTURE MEASUREMENT WITH SINGLE FIBER LOOP

Fig. 10 illustrates the setup measuring current on a large aluminum cylinder that simulates an aircraft fuselage. Currents from 250 A to 4 kA (limited by the lightning waveform generator) were injected onto the cylinder on the left side (bottom), and return currents were extracted from the right side (bottom). A single fiber loop was used, with both ends co-routed to the optical box on the table in the foreground. A Pearson CT and a Rogowski coil provide reference data for comparison. Fig.

11 shows good results for both 250 A and 4 kA cases. Noise is clearly visible in 250 A peak measurement.

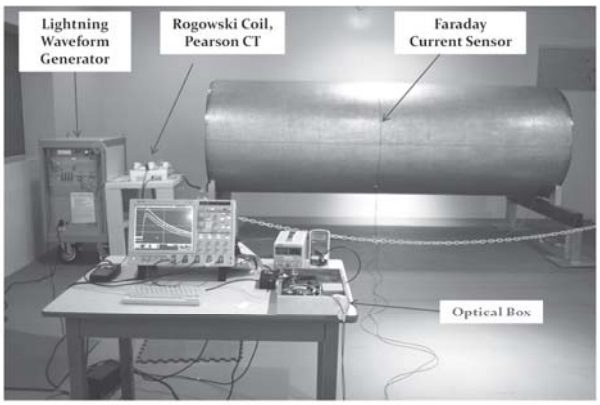

Fig. 10. Measurement on a large aluminum cylinder simulating an aircraft fuselage.

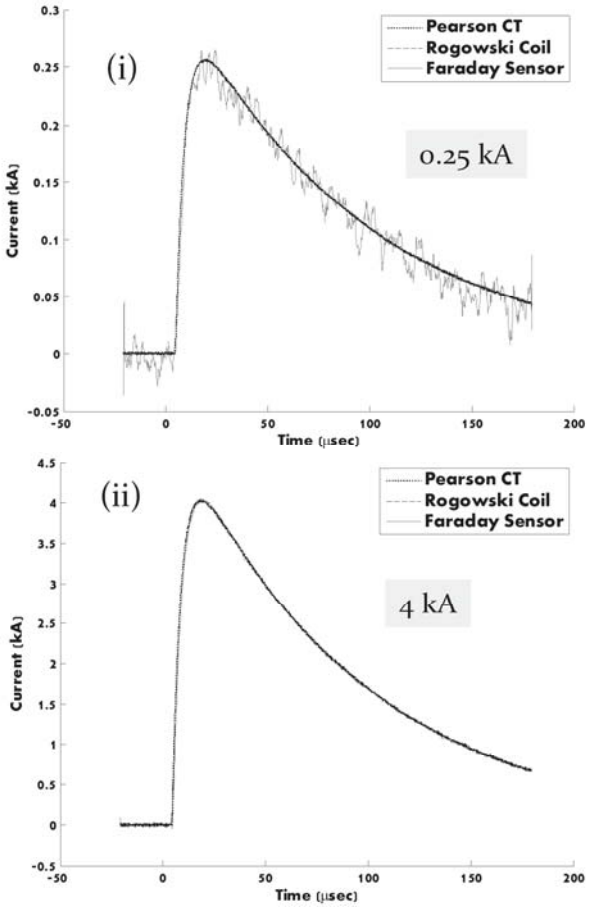

Fig. 11. Measurement on the aluminum cylinder using one fiber loop.

INTERNAL STRUCTURE MEASUREMENT

In Fig. 12, the Faraday sensor measures current flowing on an internal structure (aluminum box with square cross section) in presence of larger current flowing on the outside cylinder (i.e. aircraft fuselage). 2 kA peak current, measured with a Rogowski coil, was injected onto the cylinder. Some current was tapped-off at the coupling location and routed to the metal box, then exited at the back on the cylinder. A Pearson CT provided comparison reference data measuring current on the cable connecting the box to the coupling junction.

The Faraday sensor formed one loop around the square box. Both ends of the fiber loop were co-routed away to the optical box located about 4 meters from the cylinder (Fig. 10). The measured peak current on the box was about 140 A. The comparison was very good, even though the Faraday sensor was operating near its low end

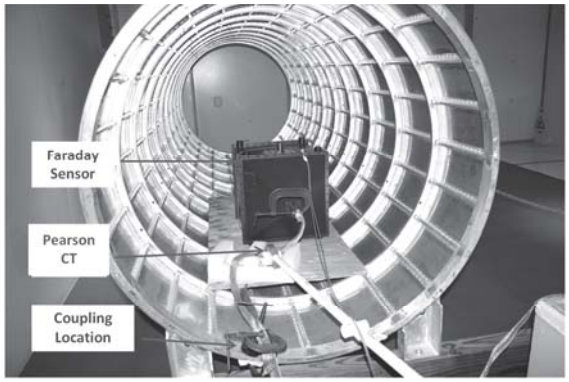

Fig. 12. Measuring current on a simulated internal structure.

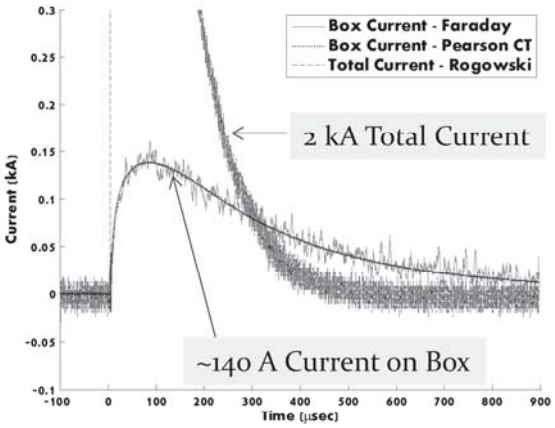

Fig. 13. Measuring current on a simulated aircraft internal structure. Good result comparison between Faraday sensor and Pearson CT.

limit and its data were noisy. This setup and the results illustrate the sensor's ability to conform to an arbitrary shape (square box), and the ability to isolate and perform low level measurement in presence of strong ambient fields.

The setup for data in Fig. 14 is similar to Fig. 12, but with the fiber loop expanded and attach to the entire inside circumference of the cylinder. A total of 4 kA were injected into the setup, about 1.5 kA flowed through the internal box. The Faraday sensor measured total internal current enclosed by the loop, while Pearson CT measured current on the cable leading to the box. Again, excellent comparison was achieved between the Faraday sensor and the Pearson CT. This again demonstrates the ability to isolate from nearby strong current and to measure only current enclosed by the large fiber loop.

This setup illustrates a potential new capability: to measure the *total* lightning-induced internal current on all wire bundles and internal structures. This capability could be useful in certification testing (i.e., providing coupling data upper bounds), or in aircraft maintenance (i.e., to signal current surge level for protection devices maintenance). With the sensor being non-intrusive, small and conformal, installation for these purposes would be simple, even on existing aircraft.

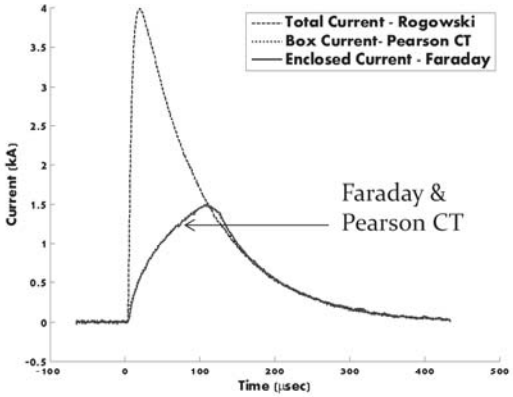

Fig. 14. Measuring total internal current using a large fiber loop. 4 kA current was injected onto to cylinder.

CONCLUSION

Accuracy of fiber-optic Faraday sensor is demonstrated measuring lightning current external and internal to a simulated aircraft fuselage. Large current measurement is also demonstrated. With multiple unique characteristics, this sensor provides new lightning current measurement capabilities, and may open new applications in aircraft lightning detection, measurement and certification areas.

REFERENCES

[1] F. L. Pitts, B. D. Fisher, V. Mazur, and R. A. Perala, "Aircraft Jolts from Lightning Bolts," IEEE Spectrum, July 1988.

[2] S. G. M. Krämer, and F. P. León, "Fiber-Optic Current Sensors for Lightning Detection in Wind Turbines," OSA/OFS, 2006.

[3] S. Alestra, I. Revel, V. Srithammavanh, M. Bardet, R. Zwemmer, D. Brown, N. Marchand, J. Ramos, V. Stelmashuk, V. "Developing an In-Flight Lightning Strike Damage Assessment System," Int. Conf. on Lightning and Static Electricity (ICOLSE), 2007.

[4] T.X. Nguyen, J.J. Ely, G.N. Szatkowski, C.T. Mata, A.G Mata, and G.P. Snyder, "Fiber-Optic Current Sensor Validation with Triggered Lightning Measurements," ICOLSE, 2013.

[5] J. M. Lopex-Higuera, Editor. Handbook of Optical Fibre Sensing Technology, 2002; Sections 27.2 - 27.4.

[6] P. Drexler and P. Fiala,"Utilization of Faraday Mirror in Fiber Optic Current Sensors", Radioengineering, Vol. 17, Dec. 2008.

[7] R.I. Laming and D.N. Payne, "Electric Current Sensors Employing Spun Highly Birefringent Optical Fibers," Journal of Lightwave Technology, Dec. 1989.

[8] G. W. Day, and A. H. Rose, "Faraday Effect Sensors: The State of the Art," Proc. SPIE, 1988, pp. 138–150.

[9] A.D. White, G.B. McHale, D.A. Goerz, "Advances in Optical Fiber-Based Faraday Rotation Diagnostics," 17th IEEE Int. Pulsed Power Conference, Wash. DC, July 2009 (LLNL-CONF-415198).

[10] T. X. Nguyen, and G. N. Szatkowski, "Fiber Optic Sensor for Aircraft Lightning Current Measurement", ICOLSE, 2011.

[11] ARP-5412 "Aircraft Lightning Environment and Related Test Waveforms," Rev B, Jan 2012.